

Supporting Information For

Insights into the effect of surface ligands on the optical properties of thiolated Au₂₅ nanoclusters

Xun Yuan, Nirmal Goswami, Weiliang Chen, Qiaofeng Yao, and Jianping Xie*

Department of Chemical and Biomolecular Engineering, National University of Singapore, 4 Engineering Drive 4, 117585, Singapore; Tel: +65 6516 1067; E-mail: chexiej@nus.edu.sg

EXPERIMENTAL SECTION

Materials and Instrumentation. Ultrapure Millipore water (18.2 MΩ) was used throughout the study unless stated. All glassware was washed with *aqua regia*, and rinsed with ethanol and ultrapure water. All chemicals were commercially available and used as received without further purification. Sodium hydroxide (NaOH) from *Merck Chemicals*; 2-mercaptoethanol (MetH) from *Bio-Rad Laboratories*; 3-mercaptopropionic acid (MPA), 6-mercaptophexanoic acid (MHA), 4-mercapto-1-butanol (MBT), 8-mercaptooctanoic acid (MOA), 11-mercaptoundecanoic acid (MUA), 2,2'-(ethylenedioxy)diethanethiol (EDT), 1,8-octanedithiol (ODT), L-cysteine (Cys), cysteamine hydrochloride (Cystm), sodium borohydride (NaBH₄) from *Sigma-Aldrich*; Hydrogen tetrachloroaurate (III) hydrate (HAuCl₄·3H₂O) from *Alfar Aesar*; were used as received.

UV-Vis absorption spectra were recorded in a *Shimadzu* UV-1800 spectrometer. Electrospray ionization mass spectrometry (ESI-MS) was performed using *Bruker* MicroTOF-Q ESI time-of-flight system operating in the negative ion mode (sample injection rate 300 μL·min⁻¹; capillary voltage 4 kV; nebulizer 1.5 bar; dry gas 4 L·min⁻¹ at 160 °C and *m/z* 100–4000). Transmission electron microscopy (TEM) images were taken on a *JEOL* JEM 2010 microscope operating at 200 kV. A stirred ultrafiltration cell (Model 8010,

Millipore Corporation, USA) with semi-permeated membranes (3 K and 20 K MWCO) were used for the purification of samples before characterization.

Synthesis of Mono-Thiolate-Protected Au₂₅ NCs. Aqueous stock solutions of HAuCl₄ (20 mM), MHA (5 mM), and NaOH (1 M) were prepared using ultrapure water. In particular, NaBH₄ solution was prepared by dissolving 43 mg of NaBH₄ powder in 10 mL of 0.2 M NaOH solution. In a typical synthesis of Au₂₅ NCs, aqueous solutions of HAuCl₄ (250 μL, 20 mM) and MHA (2 mL, 5 mM) were mixed in ultrapure water (2.4 mL) under mild stirring, followed by the addition of 250 μL of NaOH solution (1 M). The solution color was observed to fade from yellow to pale yellow. After that, 100 μL of NaBH₄ solution (20 mM) was added dropwise to the mixture and the solution color was changed to yellowish-brown. After ~3 h, high-quality Au₂₅(MHA)₁₈ NCs were collected. Various mono-thiolate-protected Au₂₅ NCs were synthesized by simply replacing the ligand MHA with other ligands like Cys, MPA, MOA, or MUA.

Synthesis of Bi-Thiolate-Protected Au₂₅ NCs. Bi-thiolate-protected Au₂₅ NCs were synthesized by keeping all the experimental conditions unchanged except for the introduction of the second thiolate ligand. Particularly, MHA (5 mM) and MetH (5 mM) were both added while keeping the volume of ligands in the sample at 2 mL. By varying the proportion of the two thiolate ligands used in the synthesis of bi-thiolate-protected Au₂₅ NCs samples (e.g., MHA/MetH = 1.25/0.75, 1.0/1.0, or 0.75/1.25), Au₂₅ NCs with different ligand proportions were obtained.

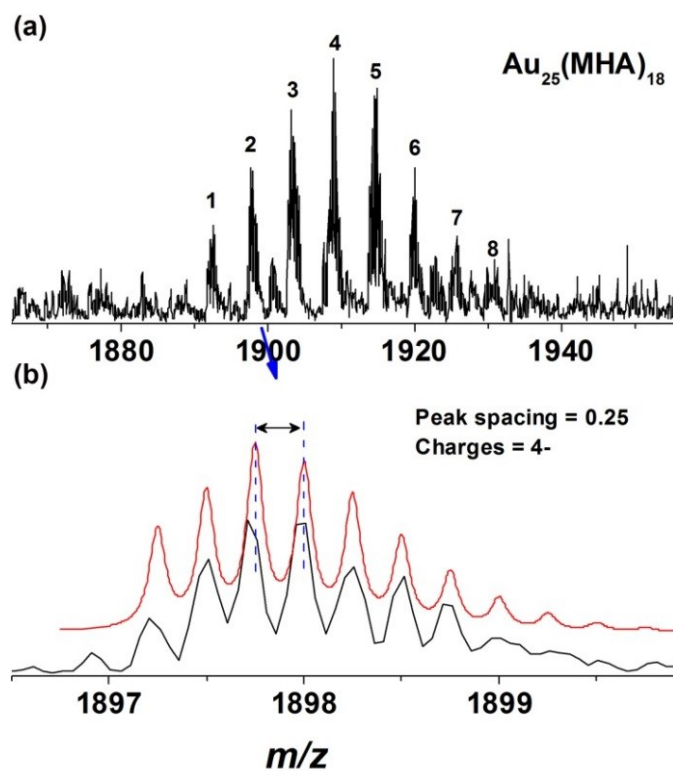


Fig. S1 (a) Zoom-in ESI mass spectrum of the as-synthesized $\text{Au}_{25}(\text{MHA})_{18}$ NCs. (b) Isotope patterns acquired theoretically (red curve) and experimentally (black curve) for the species $[\text{Au}_{25}(\text{MHA})_{18} - 5\text{H} + \text{Na}]^{4-}$. In Fig. S1a, peak #1 corresponds to $[\text{Au}_{25}(\text{MHA})_{18} - 4\text{H}]^{4-}$, and the other peaks (#2–#8) are from the successive coordination of $[+ \text{Na} - \text{H}]$ of peak #1.

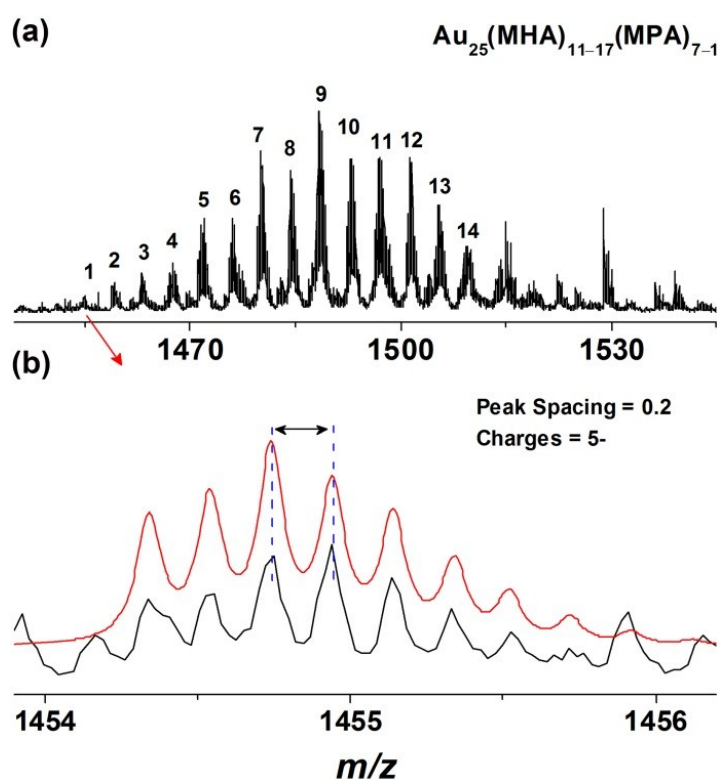


Fig. S2 (a) Zoom-in ESI mass spectrum of the as-synthesized $\text{Au}_{25}(\text{MHA})_{11-17}(\text{MPA})_{7-1}$ NCs. (b) Isotope patterns acquired theoretically (red curve) and experimentally (black curve) for the species $[\text{Au}_{25}(\text{MHA})_{11}(\text{MPA})_7 - 5\text{H}]^{5-}$. In Fig. S2a, peak #1 corresponds to $[\text{Au}_{25}(\text{MHA})_{11}(\text{MPA})_7 - 5\text{H}]^{5-}$, peaks #3, #5, #7, #9, and #11 are from the successive coordination of [+ MHA - MPA] of peak #1, and the other peaks #2, #4, #6, #8, #10, and #12–#14 are from the successive coordination of [+ Na - H] of the previous peak.

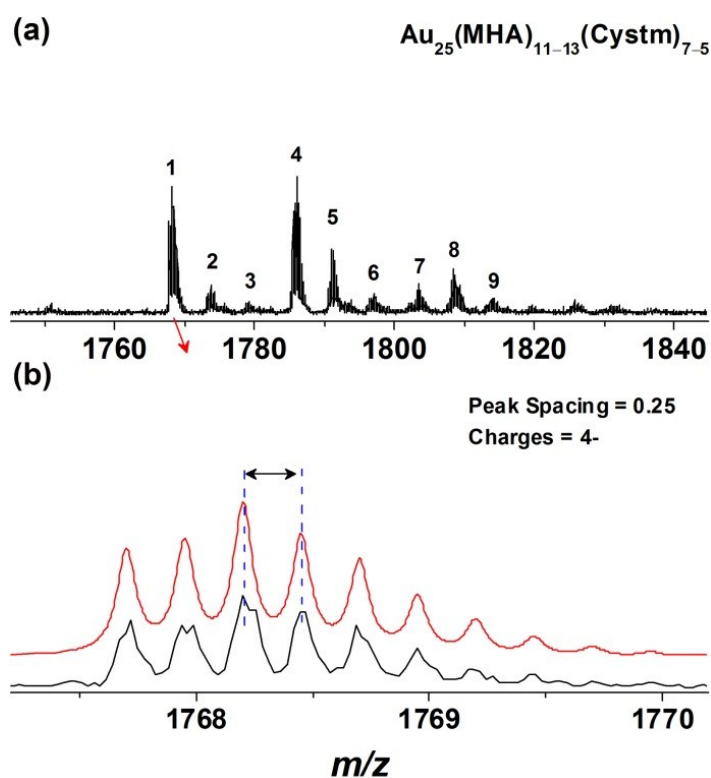


Fig. S3 (a) Zoom-in ESI mass spectrum of the as-synthesized $\text{Au}_{25}(\text{MHA})_{11-13}(\text{Cystm})_{7-5}$ NCs. (b) Isotope patterns acquired theoretically (red curve) and experimentally (black curve) for the species $[\text{Au}_{25}(\text{MHA})_{11}(\text{Cystm})_7 - 3\text{H}]^{4-}$. In Fig. S3a, peak #1 corresponds to $[\text{Au}_{25}(\text{MHA})_{11}(\text{Cystm})_7 - 3\text{H}]^{4-}$, peaks #4 and #7 are from the successive coordination of $[+\text{MHA} - \text{Cystm}]$ of peak #1, and the other peaks #2–3, #5–6, and #8–9 are from the successive coordination of $[+\text{Na} - \text{H}]$ of the previous peak.

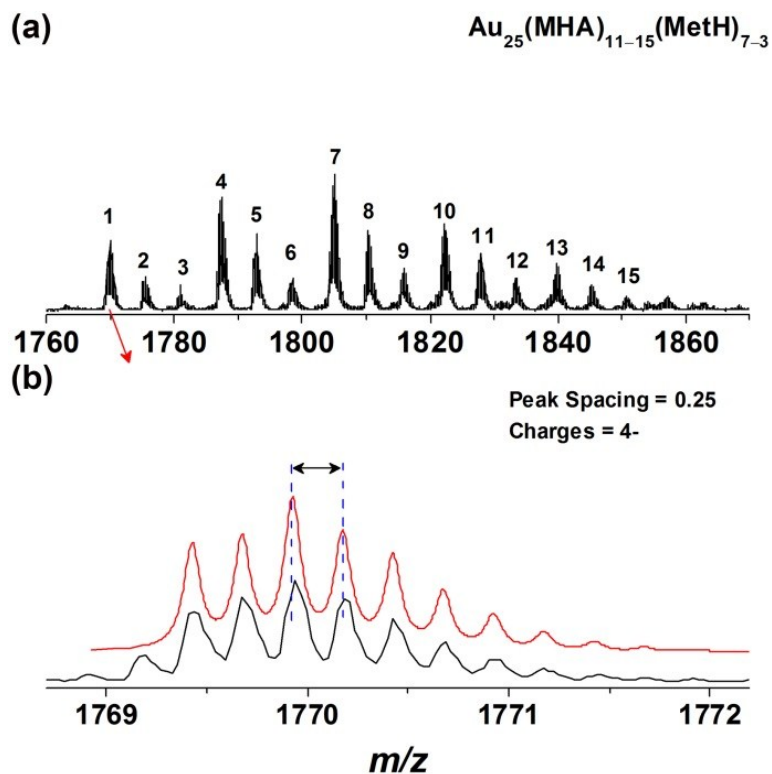


Fig. S4 (a) Zoom-in ESI mass spectrum of the as-synthesized $\text{Au}_{25}(\text{MHA})_{11-15}(\text{MetH})_{7-3}$ NCs. (b) Isotope patterns acquired theoretically (red curve) and experimentally (black curve) for the species $[\text{Au}_{25}(\text{MHA})_{11}(\text{MetH})_7 - 3\text{H}]^{4-}$. In Fig. S4a, peak #1 corresponds to $[\text{Au}_{25}(\text{MHA})_{11}(\text{MetH})_7 - 3\text{H}]^{4-}$, and peaks #4, #7, #10, and #13 are from the successive coordination of [+ MHA - MetH] of peak #1, and the other peaks #2–3, #5–6, #8–9, #11–12, and #14–15 are from the successive coordination of [+ Na - H] of the previous peak.

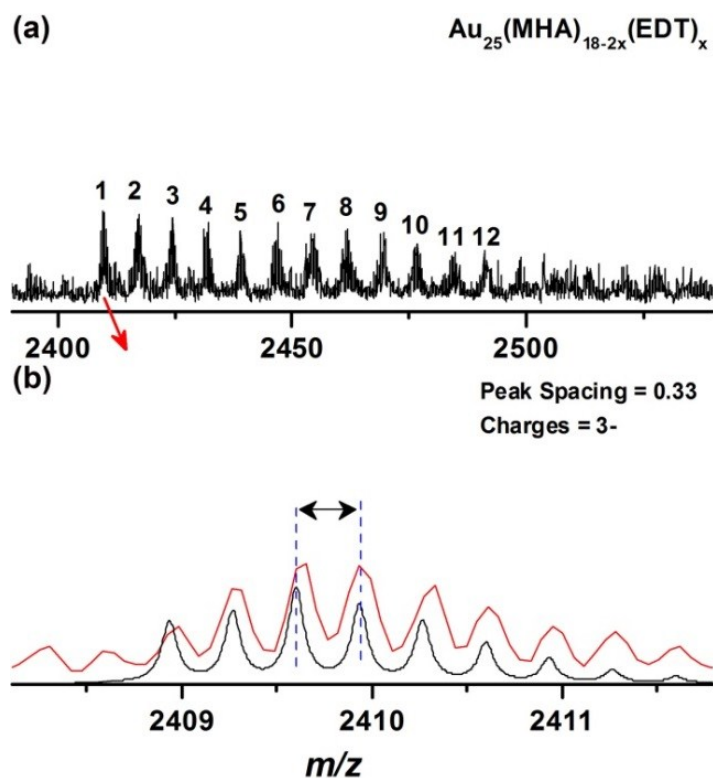


Fig. S5 (a) Zoom-in ESI mass spectrum of the as-synthesized $\text{Au}_{25}(\text{MHA})_{18-2x}(\text{EDT})_x$ NCs (here $x = 3, 2,$ and 1). (b) Isotope patterns acquired theoretically (red curve) and experimentally (black curve) for the species $[\text{Au}_{25}(\text{MHA})_{12}(\text{EDT})_3 - 2\text{H}]^{3-}$. In Fig. S5a, peak #1 corresponds to $[\text{Au}_{25}(\text{MHA})_{12}(\text{EDT})_3 - 2\text{H}]^{3-}$, peaks #6 and #11 are from the successive coordination of $[+ 2\text{MHA} - \text{EDT}]$ of peak #1, and the other peaks #2–5, #7–10, and #12 are from the successive coordination of $[+ \text{Na} - \text{H}]$ of the previous peak.

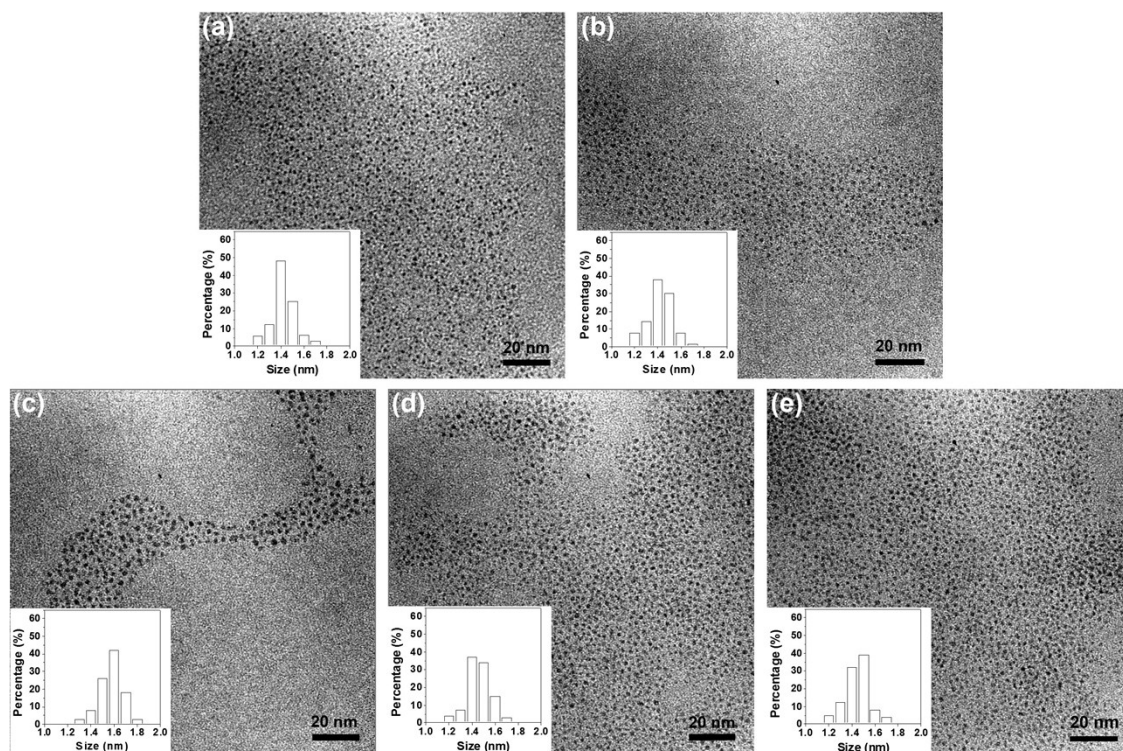


Fig. S6 Representative TEM images of the as-synthesized (a) Au₂₅(MHA)₁₈, (b) Au₂₅(MHA)₁₁₋₇(MPA)₇₋₁, (c) Au₂₅(MHA)₁₁₋₁₃(Cyst)₇₋₅, (d) Au₂₅(MHA)₁₁₋₁₅(MetH)₇₋₃, and (e) Au₂₅(MHA)_{18-2x}(EDT)_x NCs (here x = 3, 2, and 1). Insets are size histograms.

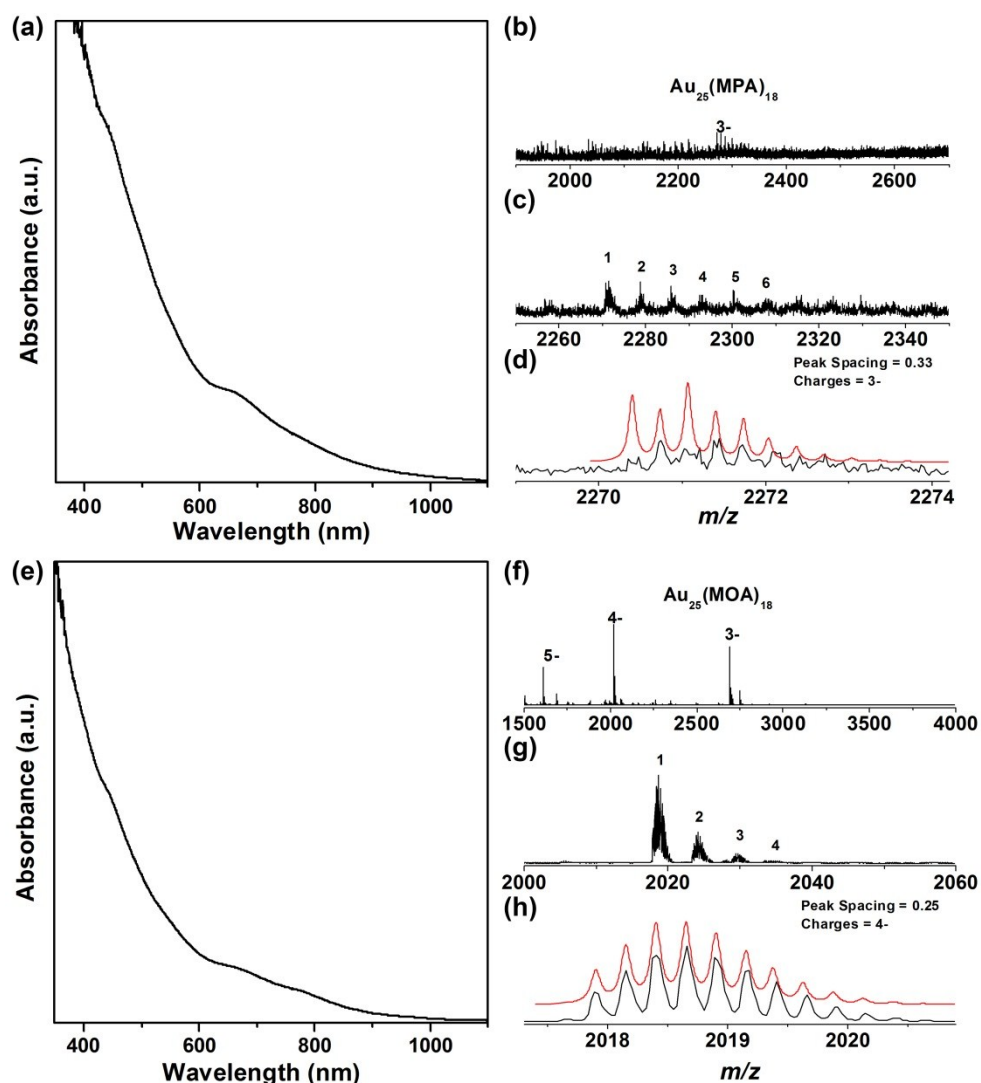


Fig. S7 (a) UV-Vis absorption spectrum, (b) ESI mass spectrum, (c) Zoom-in ESI mass spectrum of $\text{Au}_{25}(\text{MPA})_{18}$ NCs, and (d) Isotope patterns acquired theoretically (red curve) and experimentally (black curve) for the species $[\text{Au}_{25}(\text{MPA})_{18} - 3\text{H}]^{3-}$; (e) UV-Vis absorption spectrum, (f) ESI mass spectrum, (g) Zoom-in ESI mass spectrum of $\text{Au}_{25}(\text{MOA})_{18}$ NCs, and (h) Isotope patterns acquired theoretically (red curve) and experimentally (black curve) for the species $[\text{Au}_{25}(\text{MOA})_{18} - 4\text{H}]^{4-}$. Peaks #2–#6 shown in Fig. S7c, and peaks #2–#4 shown in Fig. S7g are from the successive coordination of $[\text{+Na} - \text{H}]$ of peak #1.

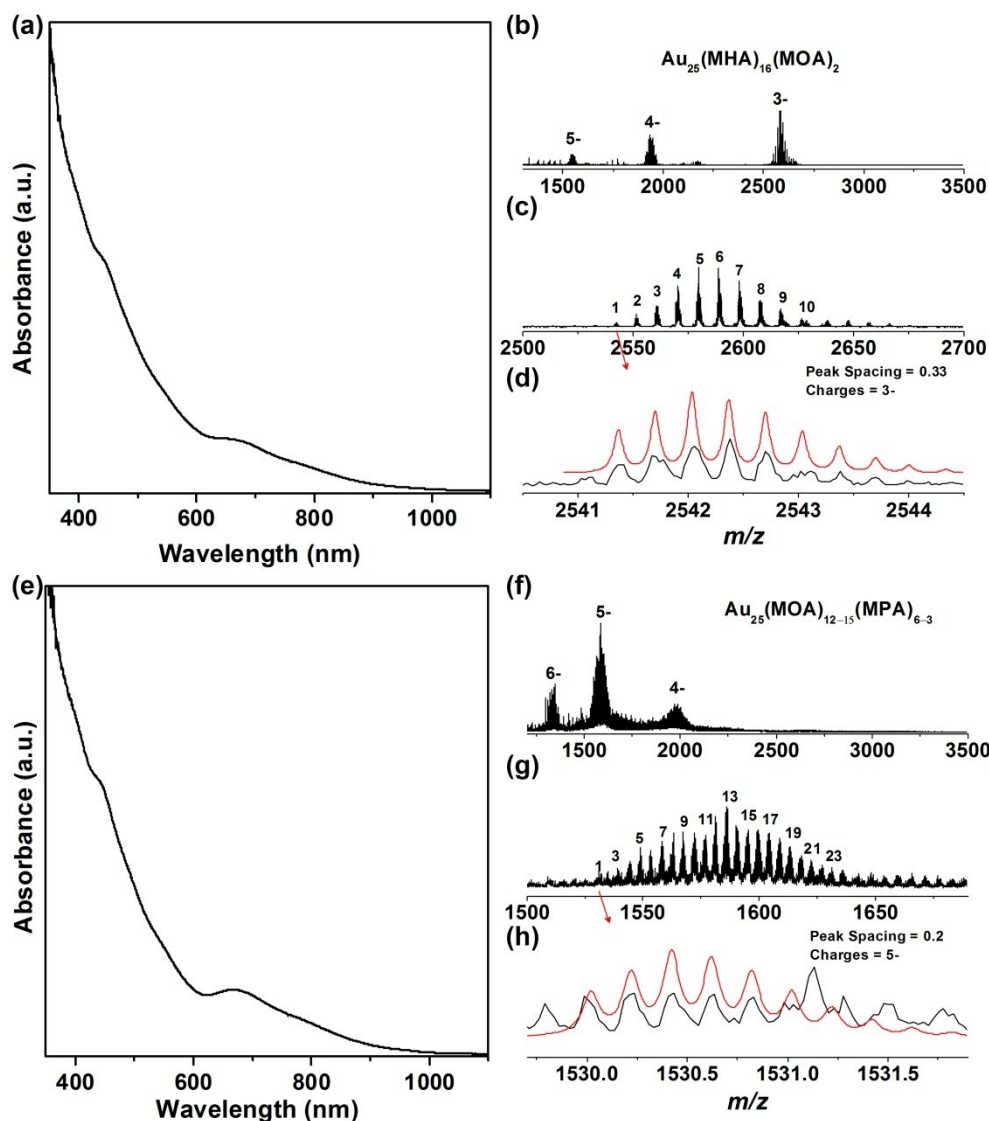


Fig. S8 (a) UV-Vis absorption spectrum, (b) ESI mass spectrum, (c) Zoom-in ESI mass spectrum of $\text{Au}_{25}(\text{MHA})_{16}(\text{MOA})_2$ NCs, and (d) Isotope patterns acquired theoretically (red curve) and experimentally (black curve) for the species $[\text{Au}_{25}(\text{MHA})_{16}(\text{MOA})_2 - 3\text{H}]^{3-}$. Peaks #2–#10 shown in Fig. S8c are from the successive coordination of $[+\text{Na} - \text{H}]$ of peak #1. (e) UV-Vis absorption spectrum, (f) ESI mass spectrum, (g) Zoom-in ESI mass spectrum of $\text{Au}_{25}(\text{MOA})_{12-15}(\text{MPA})_{6-3}$ NCs, and (h) Isotope patterns acquired theoretically (red curve) and experimentally (black curve) for the species $[\text{Au}_{25}(\text{MOA})_{12}(\text{MPA})_6 - 5\text{H}]^{5-}$. In Fig. S8g, peak #1 corresponds to $[\text{Au}_{25}(\text{MOA})_{12}(\text{MPA})_6 - 5\text{H}]^{5-}$, peaks #4, #7, and #10 are from the successive coordination of $[+\text{MOA} - \text{MPA}]$ of peak #1, and the other peaks #2–3, #5–6, #8–9, and #11–24 are from the successive coordination of $[+\text{Na} - \text{H}]$ of the previous peak.

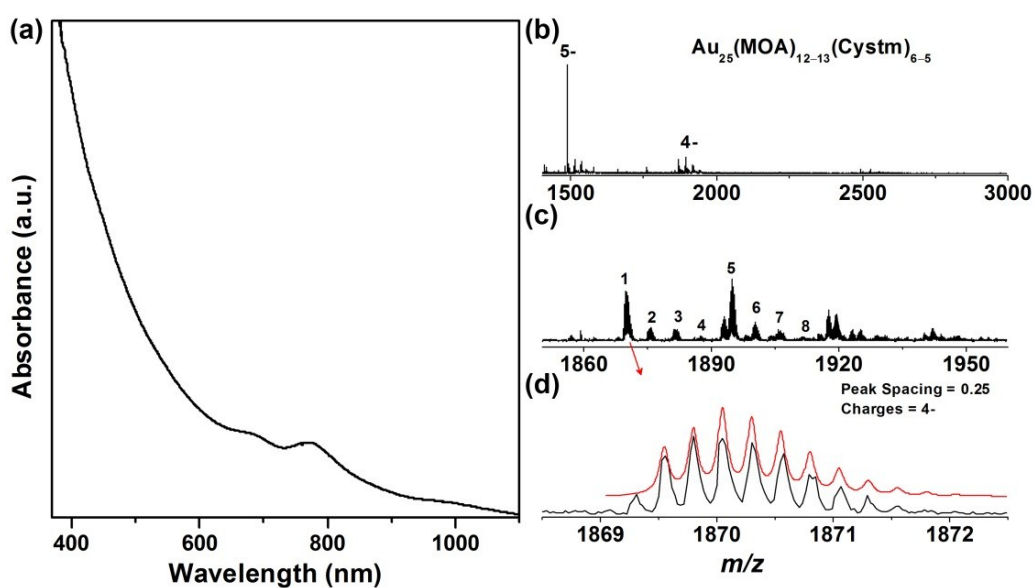


Fig. S9 (a) UV-Vis absorption spectrum, (b) ESI mass spectrum, (c) Zoom-in ESI mass spectrum of $\text{Au}_{25}(\text{MOA})_{12-13}(\text{Cystm})_{6-5}$ NCs, and (d) Isotope patterns acquired theoretically (red curve) and experimentally (black curve) for the species $[\text{Au}_{25}(\text{MOA})_{12}(\text{Cystm})_6 - 3\text{H}]^{4-}$. In Fig. S9c, peak #1 and #5 corresponds to $[\text{Au}_{25}(\text{MOA})_{12}(\text{Cystm})_6 - 3\text{H}]^{4-}$ and $[\text{Au}_{25}(\text{MOA})_{13}(\text{Cystm})_5 - 3\text{H}]^{4-}$, respectively, and the other peaks #2–#4, and #6–#8 are from the successive coordination of $[+ \text{Na} - \text{H}]$ of the previous peak.

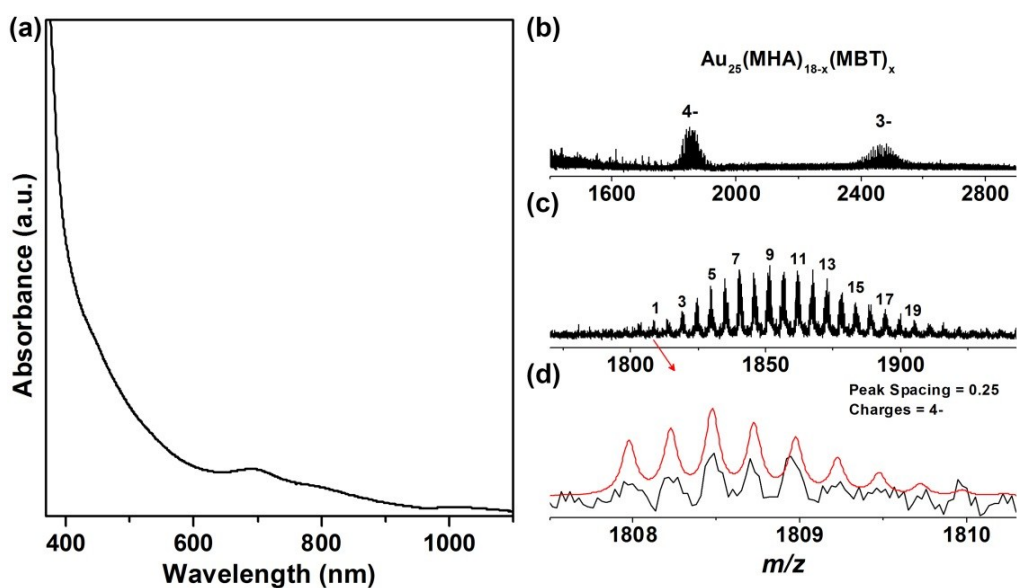


Fig. S10 (a) UV-Vis absorption spectrum, (b) ESI mass spectrum, (c) Zoom-in ESI mass spectrum of $\text{Au}_{25}(\text{MHA})_{18-x}(\text{MBT})_x$ NCs (here $x = 8$ and 4), and (d) Isotope patterns acquired theoretically (red curve) and experimentally (black curve) for the species $[\text{Au}_{25}(\text{MHA})_{10}(\text{MBT})_8 - 3\text{H}]^{4-}$. In Fig. S10c, peak #1 and #9 corresponds to $[\text{Au}_{25}(\text{MHA})_{10}(\text{MBT})_8 - 3\text{H}]^{4-}$ and $[\text{Au}_{25}(\text{MHA})_{14}(\text{MBT})_4 - 3\text{H}]^{4-}$, respectively, and the other peaks #2–#8, and #10–#19 are from the successive coordination of $[\text{Na} - \text{H}]$ of the previous peak.

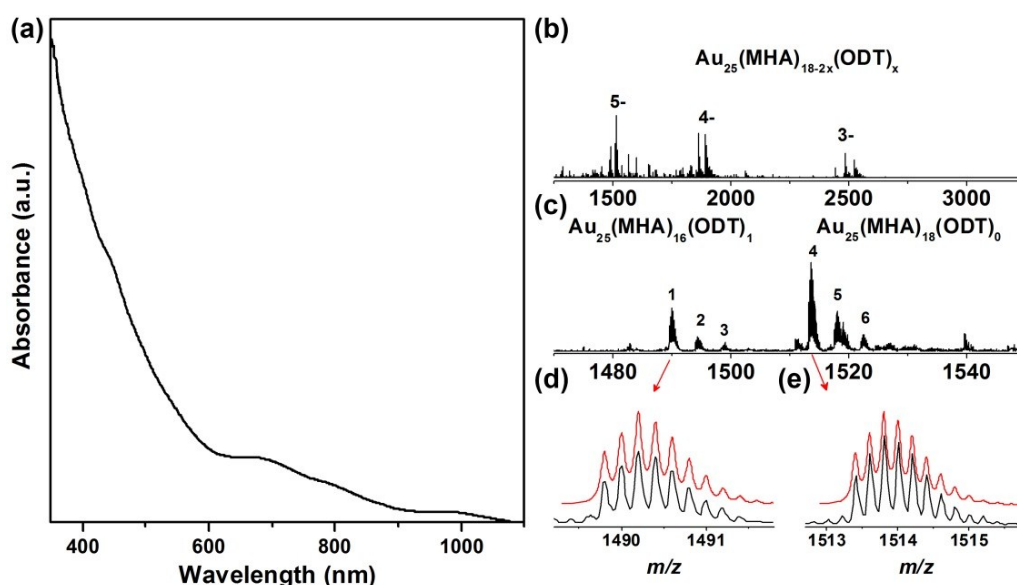


Fig. S11 (a) UV-Vis absorption spectrum, (b) ESI mass spectrum, (c) Zoom-in ESI mass spectrum of $\text{Au}_{25}(\text{MHA})_{18-2x}(\text{ODT})_x$ (here $x = 1$ and 0) NCs, and (d, and e) Isotope patterns acquired theoretically (red curve) and experimentally (black curve) for the species (d) $[\text{Au}_{25}(\text{MHA})_{16}(\text{ODT})_1 - 4\text{H}]^{5-}$ and (e) $[\text{Au}_{25}(\text{MHA})_{18}(\text{ODT})_0 - 4\text{H}]^{5-}$. Peaks #2–3 and peaks #5–6 shown in Fig. S11c are from the successive coordination of $[\text{+Na} - \text{H}]$ of peak #1 and peak #4, respectively.

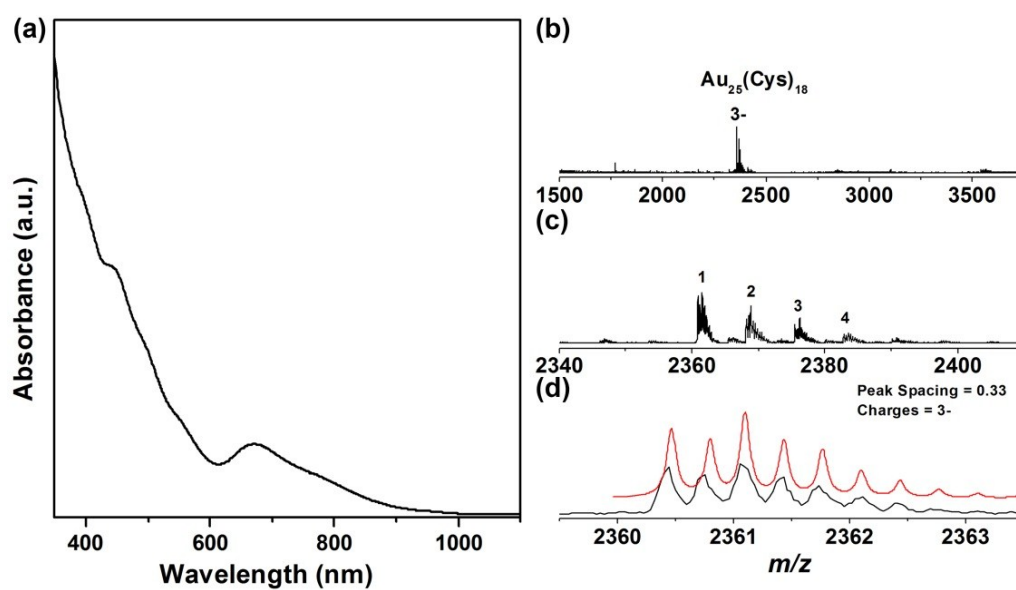


Fig. S12 (a) UV-Vis absorption spectrum, (b) ESI mass spectrum, (c) Zoom-in ESI mass spectrum of $\text{Au}_{25}(\text{Cys})_{18}$ NCs, and (d) Isotope patterns acquired theoretically (red curve) and experimentally (black curve) for the species $[\text{Au}_{25}(\text{Cys})_{18} - 3\text{H}]^{3-}$. Peaks #2–#4 shown in Fig. S12c are from the successive coordination of $[\text{+Na} - \text{H}]$ of peak #1.

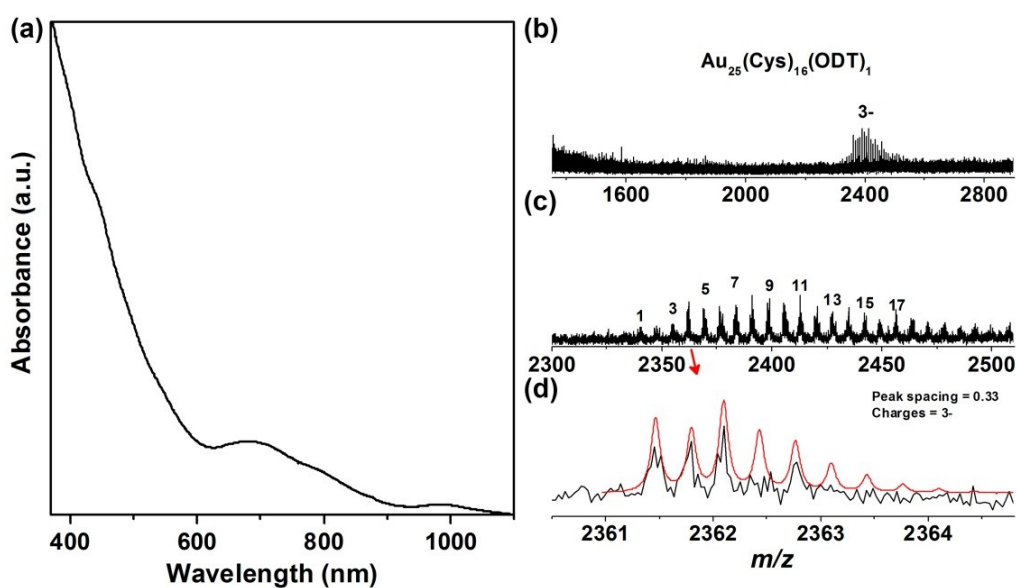


Fig. S13 (a) UV-Vis absorption spectrum, (b) ESI mass spectrum, (c) Zoom-in ESI mass spectrum of $\text{Au}_{25}(\text{Cys})_{16}(\text{ODT})_1$ NCs, and (d) Isotope patterns acquired theoretically (red curve) and experimentally (black curve) for the species $[\text{Au}_{25}(\text{Cys})_{16}(\text{ODT})_1 - 5\text{H} + 3\text{Na}]^{3-}$. Peaks #2–#17 shown in Fig. S13c are from the successive coordination of $[+\text{Na} - \text{H}]$ of peak #1.

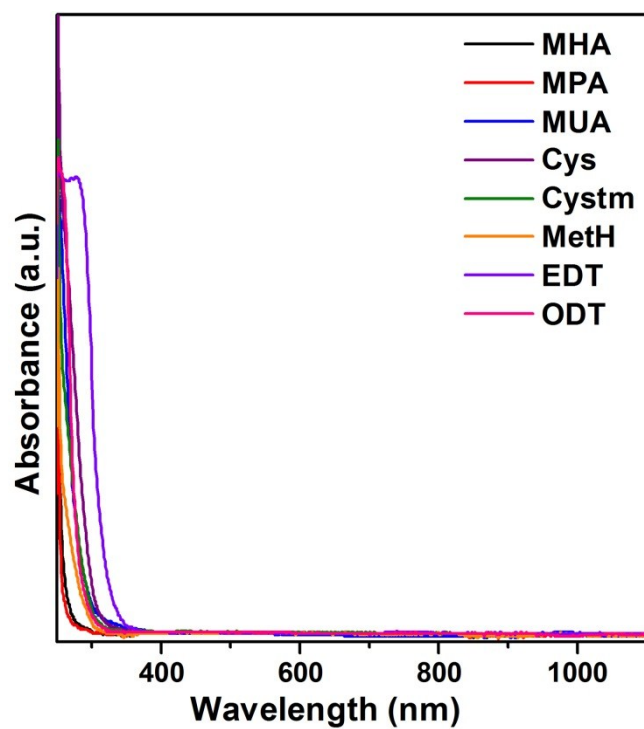


Fig. S14 UV-Vis absorption spectra of all the ligands used in the synthesis of thiolated Au₂₅ NCs. No absorption peak at ~980 nm could be seen.

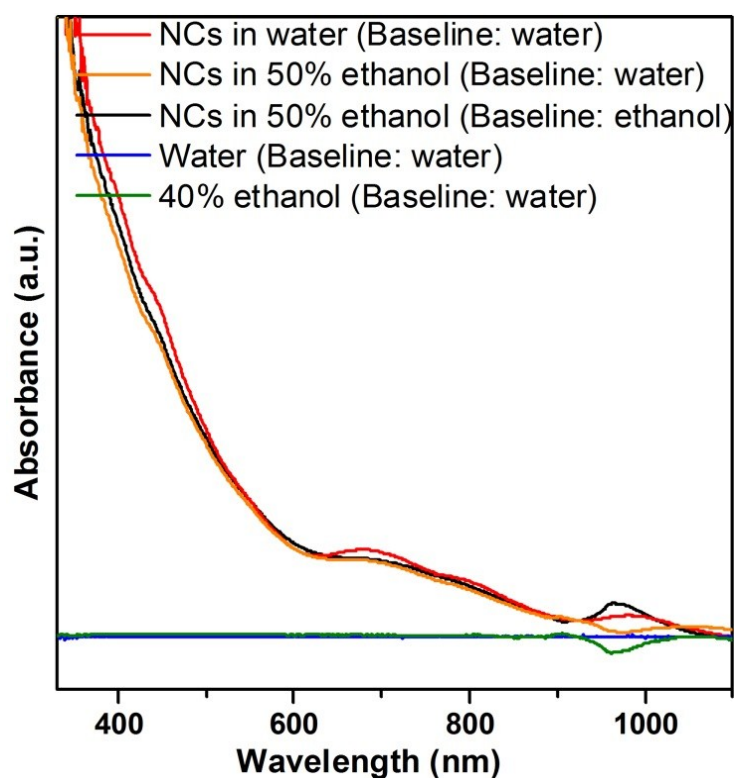


Fig. S15 UV-Vis absorption spectra of MHA/Cystm-protected Au₂₅ NCs dissolved in water (red curve; ultrapure water is used as baseline), and in mixed solvent of water and ethanol (volume ratio of 1/1; orange curve when ultrapure water is used as baseline, and black curve when ethanol is used as baseline), as compared to the ultrapure water (blue curve; ultrapure water is used as baseline) and mixed solvent of water and ethanol (volume ratio of 3/2; green curve; ultrapure water is used as baseline).

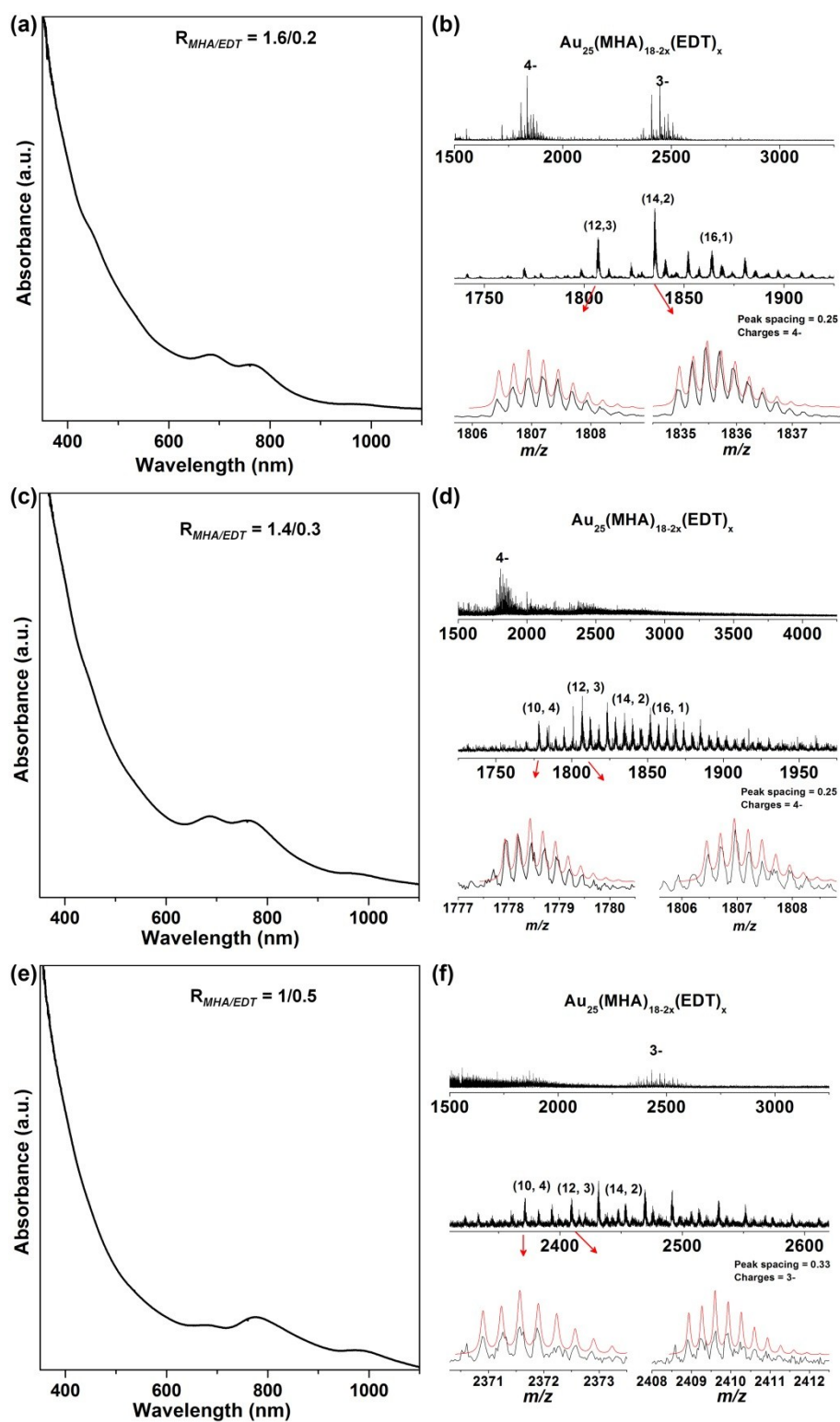


Fig. S16 UV-Vis absorption spectra (a, c, e), and ESI mass spectra (b, d, f) of bi-ligand MHA/EDT-protected Au₂₅ NCs synthesized at thiol ratios of $R_{MHA/EDT} = 1.6/0.2$, $1.4/0.3$, and $1.0/0.5$. The bottom panels in Fig. S16(b), (d) and (f) show isotope patterns acquired theoretically (red curve) and experimentally (black curve) for the Au₂₅ species: [Au₂₅(MHA)₁₂(EDT)₃ - 3H]⁴⁺, and [Au₂₅(MHA)₁₄(EDT)₂ - 3H]⁴⁺; [Au₂₅(MHA)₁₀(EDT)₄ - 3H]⁴⁺, and [Au₂₅(MHA)₁₂(EDT)₃ - 3H]⁴⁺; [Au₂₅(MHA)₁₀(EDT)₄ - 2H]³⁻, and [Au₂₅(MHA)₁₂(EDT)₃ - 2H]³⁻.